for **12–15** compared to **6–11** as the solvent is changed.

Summary and Conclusions

The presence of ortho chloro or methyl substituents on the meso phenyl groups in the six-coordinate complexes Co(TDCPP)-$(RIm)_2^+$ and Co(TMP)$(RIm)_2^+$ has a large effect on the ^{59}Co NMR chemical shifts and line widths when compared to analogous cobalt complexes lacking ortho substituents on the phenyls, e.g., Co(TPP)$(RIm)_2^+$. Extensive studies of solvent effects indicate that the TDCPP and TMP complexes do not experience specific solvation, even with small solvent molecules; the solvent influence is limited to long-range polarity effects. The TPP complexes, on the other hand, exhibit specific, short-range solvation and are able to discriminate among solvents on the basis of size. The X-ray structure of [Co(TDCPP)$(MeIm)_2$]BF_4 (**13**) shows that the ortho chloro groups effectively block the space above and below the porphyrin core. The two axial imidazole ligand planes adopt a perpendicular relative orientation, with each imidazole plane nearly eclipsing a N_p–Co–N_p bond axis. Additionally, the porphyrin core is substantially ruffled with approximate S_4 symmetry. The distortions associated with the bulky ortho groups in these hindered complexes accounts for the observed solvent dependence of the NMR parameters. Furthermore, strong evidence is presented that the electric field gradient changes sign in going from unhindered to hindered complexes. The structural results provide a ready rationale for this in terms of decreased axial and increased equatorial interaction between the cobalt d-orbitals and the ligand orbitals in the hindered complexes.

Acknowledgment. We gratefully acknowledge the expert experimental assistance of Dr. J. Van Epp and Dr. W. A. Hallows. K.R. was a participant in the NSF Research Experience for Undergraduates program at Brown University in the summer of 1989.

Supplementary Material Available: Hydrogen coordinates (Table SI) and anisotropic thermal parameters (Table SII) for [Co(TDCPP)$(MeIm)_2$]BF_4 (**13**) (3 pages); observed and calculated structure factors (Table SIII) for **13** (42 pages). Ordering information is given on any current masthead page.

Conformational Analysis of a Highly Potent, Constrained Gonadotropin-Releasing Hormone Antagonist. 1. Nuclear Magnetic Resonance

Josep Rizo,[†] Steven C. Koerber,[‡] Rachelle J. Bienstock,[†] Jean Rivier,[‡] Arnold T. Hagler,[§] and Lila M. Gierasch*,[†]

Contribution from the Department of Pharmacology, University of Texas Southwestern Medical Center, 5323 Harry Hines Boulevard, Dallas, Texas 75235-9041, Biosym Technologies, Inc., 10065 Barnes Canyon Road, San Diego, California 92121, and The Clayton Foundation Laboratories for Peptide Biology, The Salk Institute, 10010 North Torrey Pines Road, La Jolla, California 92037. *Received August 19, 1991*

Abstract: Conformational analysis of a cyclic decapeptide analogue of gonadotropin-releasing hormone (GnRH) led to the design of a series of highly potent GnRH antagonists constrained by a bridge between residues 4 and 10 (Struthers, R. S.; et al. *Proteins* **1990**, *8*, 295). We have now used nuclear magnetic resonance (NMR) to study the conformational behavior of one of the most potent of these GnRH antagonists: Ac-Δ^3-Pro1-D-*p*FPhe2-D-Trp3-c(Asp4-Tyr5-D-2Nal6-Leu7-Arg8-Pro9-Dpr10)-NH_2. Our data indicates that a β-hairpin conformation within residues 5–8, stabilized by two transannular hydrogen bonds, is the best defined feature of the molecule. This structure includes a type II′ β turn around positions 6 and 7, which has been proposed to be essential for the biological activity of GnRH. Conformational averaging is observed in the Asp4–Dpr10 bridge, most likely favored by the presence of two methylene groups. The linear part of the peptide, the tail formed by residues 1–3, is located above the ring and appears to be somewhat structured: a γ-turn around D-Trp3 is likely to exist, and a type II β turn around residues 1 and 2 could be frequently visited. However, some flexibility and sensitivity to the environment are evident in this region of the molecule. The β-hairpin conformation and the orientation of the tail above the ring correlate with the structure determined for the parent cyclic decapeptide, cyclo(Δ^3-Pro1-D-*p*ClPhe2-D-Trp3-Ser4-Tyr5-D-Trp6-NMeLeu7-Arg8-Pro9-β-Ala10) (Baniak, E. L., II; et al. *Biochemistry* **1987**, *26*, 2642). The conformational model emerging from the NMR data, in combination with our molecular dynamics analysis (see following paper in this issue), suggests additional bridging possibilities to obtain new, more constrained GnRH antagonists.

The last decades have witnessed the discovery of a wide variety of small peptides that modulate diverse biological functions. The definition of the structural requirements for these peptides to play their biological roles is essential to understand their mechanisms of action and to design analogues with potential clinical applications. Despite the variety of biophysical techniques that can be applied to the study of the conformational behavior of these peptides,[1] their analysis is usually hampered by their flexibility and sensitivity to the environment, characteristics that can often be necessary for their function. Perhaps the most sensitive approach to overcome this problem is the design, synthesis, and study of conformationally constrained analogues of the native peptides, which can lead to the definition of the conformational requirements for binding to the corresponding receptor(s), and for agonist or antagonist activity.[2,3]

[†] University of Texas Southwestern Medical Center.
[‡] The Salk Institute.
[§] Biosym Technologies, Inc.

(1) See, for instance *The Peptides: Analysis, Synthesis, Biology*; Udenfriend, S., Meienhofer, J., Hruby, V. J., Eds.; Academic Press: Orlando, FL, 1985; Vol. 7.

0002-7863/92/1514-2852$03.00/0

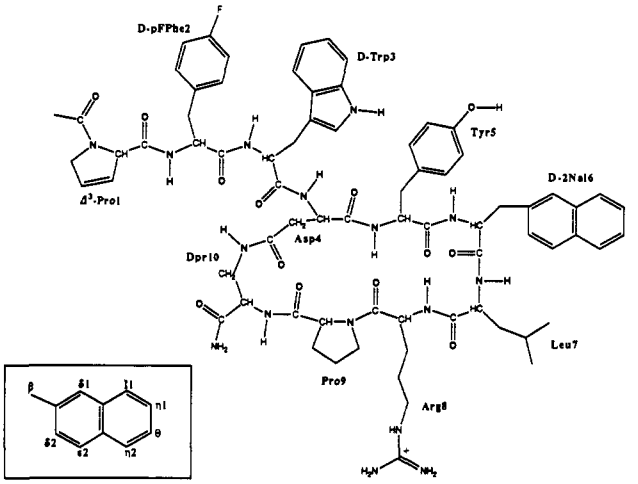

Figure 1. Schematic representation of the Asp4–Dpr10 GnRH analogue. Nomenclature and abbreviations for amino acid residues throughout the text, in one- or three-letter code, follow the recommendations of the IUPAC-IUB Commission on Biochemical Nomenclature (*Biochemistry* **1970**, *9*, 3471–3479). Other abbreviations used are as follows: *p*FPhe or F, 4-fluorophenylalanine; 2Nal or Na, 3-(2′-naphthyl)alanine; Dpr or Dp, 2,3-diaminopropionic acid. The nomenclature adopted for the positions in the aromatic ring of D-2Nal6 is indicated in the inset.

Mammalian gonadotropin-releasing hormone (GnRH), pGlu1-His2-Trp3-Ser4-Tyr5-Gly6-Leu7-Arg8-Pro9-Gly10-NH_2, is a linear decapeptide with the conformational characteristics of peptidic hormones described above: it has been found to be mainly unstructured in three different environments by nuclear magnetic resonance (NMR).[4] Due to its key role in the regulation of ovulation and spermatogenesis,[5] GnRH has been the object of intense efforts in analogue design, with the aim to develop nonsteroidal contraceptive or fertility agents.[6] Most of the nearby 3000 GnRH analogues synthesized so far are linear peptides that were developed following classical analogue design strategies, i.e., strategies where substitutions and deletions are introduced to vary the steric and hydrophobic/hydrophilic characteristics of each residue in the sequence, building on results obtained in previous modifications. However, Rivier and co-workers have succeeded in the development of highly potent GnRH antagonists constrained by cyclization.[3,7] Molecular dynamics, energy minimization, and template forcing techniques[8] were used to study a slightly active cyclic GnRH antagonist, cyclo(Δ³-Pro1-D-*p*ClPhe2-D-Trp3-Ser4-Tyr5-D-Trp6-NMeLeu7-Arg8-Pro9-β-Ala10), and a single family of conformations with close proximity between the Cα positions of Ser4 and Pro9 was identified.[9] This observation was confirmed by nuclear magnetic resonance spectroscopy[10] and led to the synthesis of 4–9 bridged analogues that had receptor affinities comparable to that of the parent cyclic decapeptide.[3] On the basis of earlier results obtained in the GnRH agonist series,[11] and in order to probe conformational space and "fine tune" the putative binding hypothesis emerging from the parent cyclic decapeptide antagonist, a series of GnRH analogues bridging residues 4 and 10 was also synthesized. This new series of compounds showed, in general, a very significant increase in binding affinity, and perhaps more important, some of them were almost as potent as the most potent linear antagonists. Therefore, the basic cyclo(4–10) structure can be used to develop a new generation of more constrained GnRH peptides,[3] and in fact, some bicyclic compounds have already been synthesized.[7]

In order to improve our working model of the bioactive conformation of GnRH, we have used high-field NMR spectroscopy to study the structure in solution of Ac-Δ³-Pro1-D-*p*FPhe2-D-Trp3-c(Asp4-Tyr5-D-2Nal6-Leu7-Arg8-Pro9-Dpr10)-NH_2 (shown schematically in Figure 1), one the most potent analogues of the cyclo(4–10) GnRH antagonist series. Our results show that this peptide, hereafter referred to as the Asp4–Dpr10 analogue, adopts a β-hairpin structure encompassing residues 5–8, which includes a type II′ β turn with residues 6 and 7 in the corner positions and two transannular hydrogen bonds. The tail formed by residues 1–3 is oriented above the ring and appears to have some flexibility. The conformational model arising from the NMR data, in combination with our molecular dynamics analysis (see following paper in this issue), shares some similarities with the structure found for the parent cyclic decapeptide[10] and indicates additional bridging possibilities for the design of more constrained GnRH antagonists.

Experimental Procedures

Synthesis. Linear Peptide Hydrazide. The peptide was synthesized on a methylbenzhydrylamine resin (MBHA-resin) (2.0 g) containing ca. 0.8 mequiv of amino group/g. Standard protocols for *tert*-butyloxycarbonyl-protected amino acids were used.[12] In summary, the Boc group was removed with trifluoroacetic acid (60%) in CH_2Cl_2 containing 2–5% ethanedithiol for 20 min, followed by neutralization with 10% triethylamine (TEA) in CH_2Cl_2. Couplings were performed in CH_2Cl_2 or CH_2Cl_2/dimethylformamide (DMF) (1:1) using dicyclohexylcarbodiimide for 2 h or less. A 2-fold excess of protected amino acids was used. N-terminal acetylation was performed with a large excess of acetic anhydride in CH_2Cl_2 in 15 min. Hydrazinolysis of the aspartic acid β-benzyl ester was carried out at the last stage of the synthesis with a large excess of anhydrous hydrazine in CH_2Cl_2 for 48 h. After washing with MeOH and CH_2Cl_2 and drying, 3.6 g of protected peptide hydrazide MBHA-resin was obtained. The Ac-Δ³-Pro-D-*p*FPhe-D-Trp-Asp-($NHNH_2$)-Tyr(2,6-Cl_2Bzl)-D-2Nal-Leu-Arg(tosyl)-Pro-Dpr(Z)-MBHA-resin (Z = benzyloxycarbonyl) was treated with liquid HF (60 mL) at 20 °C (20 min) and 0 °C (60 min) in the presence of 5 mL of anisole. The HF was removed from the reaction vessel under vacuum, and the solid residue was triturated in anhydrous ether (100 mL) and filtered. The peptide hydrazide was extracted from the resin with 10% aqueous acetonitrile and lyophilized to yield a fluffy, crude peptide hydrazide (1.06 g) which exhibited a major peak (50%) by high-performance liquid chromatography (HPLC).

Peptide Cyclization. Crude peptide hydrazide (1.0 g, 0.7 mmol) was dissolved in 300 mL of DMF at −25 °C; 4 M HCl in dioxane (0.85 mL, 3.5 mmol) and isoamyl nitrite in three aliquots (0.15 mL, 1.0 mmol) were added with stirring over 15 min. Stirring at −25 °C was continued for 3 h. The solution of peptide azide was diluted with 600 mL of DMF

(2) (a) Veber, D. F.; Holly, F. W.; Nutt, R. F.; Bergstrand, S. J.; Brady, S. F.; Hirschmann, R.; Glitzer, M. S.; Saperstein, R. *Nature* **1979**, *280*, 512–514. (b) Hruby, V. J. *Life Sci.* **1982**, *31*, 189–199. (c) Hruby, V. J. In *The Peptides: Analysis, Synthesis, Biology*; Udenfriend, S., Meienhofer, J., Hruby, V. J., Eds.; Academic Press: Orlando, FL, 1985; Vol. 7, pp 1–14.

(3) (a) Rivier, J.; Kupryszewski, G.; Varga, J.; Porter, J.; Rivier, C.; Perrin, M.; Hagler, A.; Struthers, S.; Corrigan, A.; Vale, W. *J. Med. Chem.* **1988**, *31*, 677–682. (b) Struthers, R. S.; Tanaka, G.; Koerber, S.; Solmajer, T.; Baniak, E. L.; Gierasch, L. M.; Vale, W.; Rivier, J.; Hagler, A. T. *Proteins* **1990**, *8*, 295–304.

(4) Chary, K. V. R.; Srivastava, S.; Hosur, R. V.; Boy, K. B.; Govil, G. *Eur. J. Biochem.* **1986**, *158*, 323–332.

(5) (a) Vander, A. J.; Sherman, J. H.; Luciano, D. S. *Human Physiology, the Mechanisms of Body Function*; McGraw-Hill: New York, 1970; pp 443–471. (b) Matsuo, H.; Baba, Y.; Nair, R. M. G.; Arimura, A.; Schally, A. V. *Biochem. Biophys. Res. Commun.* **1971**, *43*, 1374–1439. (c) Burgus, R.; Butcher, M.; Amoss, M.; Ling, N.; Monahan, M.; Rivier, J.; Fellows, R.; Blackwell, R.; Vale, W.; Guillemin, R. *Proc. Natl. Acad. Sci. U.S.A.* **1972**, *69*, 278–282.

(6) (a) Vickery, B. H., Nestor, J. J., Jr., Hafez, E. S. E., Eds. *LHRH and Its Analogs: Contraceptives and Therapeutic Applications*; MTP Press: Lancaster, England, 1984. (b) Karten, M.; Rivier, J. *Endocr. Rev.* **1986**, *7*, 44–66.

(7) (a) Rivier, J.; Koerber, S.; Rivier, C.; Hagler, A.; Perrin, M.; Gierasch, L.; Corrigan, A.; Porter, J.; Vale, W. In *International Symposium on Frontiers in Reproduction Research: The Role of Growth Factors, Oncogenes, Receptors and Gonadal Polypeptides*, Beijing, China; Chen, H.-C., Ed.; in press. (b) Rivier, J. E.; Rivier, C.; Vale, W.; Koerber, S.; Corrigan, A.; Porter, J.; Gierasch, L. M.; Hagler, A. T. In *Peptides: Chemistry, Structure and Biology*; Rivier, E. J., Marshall, G. R., Eds.; ESCOM: Leiden, The Netherlands, 1990; pp 33–37.

(8) (a) Hagler, A. T. In *The Peptides: Analysis, Synthesis, Biology*; Udenfriend, S., Meienhofer, J., Hruby, V. J., Eds.; Academic Press: Orlando, FL, 1985; Vol. 7, pp 213–299. (b) Hagler, A. T.; Osguthorpe, D. J.; Dauber-Osguthorpe, P.; Hempel, J. C. *Science* **1985**, *227*, 1309–1315.

(9) (a) Struthers, R. S.; Rivier, J.; Hagler, A. T. In *Conformationally Directed Drug Design-Peptides and Nucleic Acids as Templates or Targets*; Vida, J. A., Gorden, M., Eds.; American Chemical Society: Washington, DC, 1984; pp 239–261. (b) Struthers, R. S.; Rivier, J.; Hagler, A. *Ann. N.Y. Acad. Sci.* **1985**, *439*, 81–96.

(10) Baniak, E. L., II; Rivier, J. E.; Struthers, R. S.; Hagler, A. T.; Gierasch, L. M. *Biochemistry* **1987**, *26*, 2642–2656.

(11) Rivier, J.; Rivier, C.; Perrin, M.; Porter, J.; Vale, W. In *LHRH Peptides as Female and Male Contraceptives*; Zatachni, G. I., Shelton, J. D., Sciarra, J. J., Eds.; Harper and Row: Philadelphia, PA, 1981; pp 13–23.

(12) Marki, W.; Spiess, J.; Tache, Y.; Brown, M.; Rivier, J. E. *J. Am. Chem. Soc.* **1981**, *103*, 3178–3185.

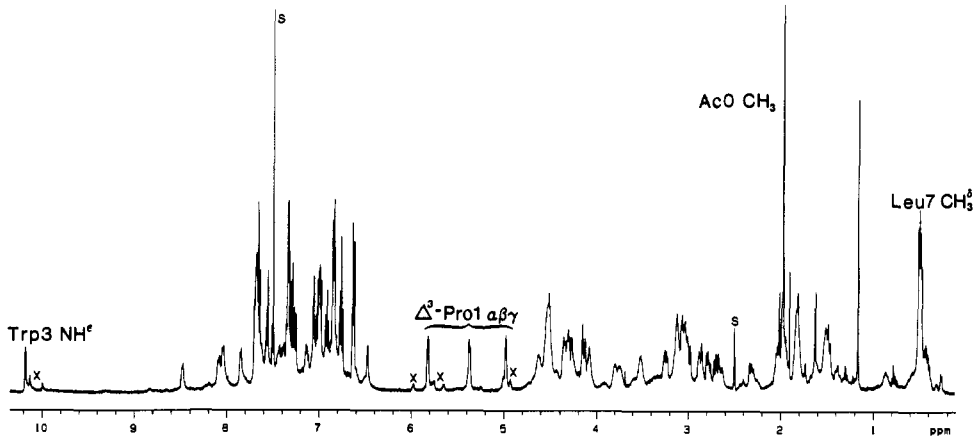

Figure 2. One-dimensional 500-MHz ^{1}H NMR spectrum of the Asp4–Dpr10 GnRH analogue in $CDCl_3$/DMSO-d_6 (5:1 (v/v)). Small signals labeled with an x indicate the presence of minor conformers accompanying the major form of the peptide. Solvent resonances are labeled with an s.

(precooled to −25 °C), and diisopropylethylamine was added until the pH on moistened pH indicator gave a value of 7.6. The solution was stored at −25 °C (24 h) and 5 °C (72 h). The solvent was evaporated under vacuum to yield crude cyclic peptide (1.0 g after lyophilization from water/acetonitrile (3:1)), which was found to be ca. 30% pure by HPLC.

Peptide Purification by Reversed-Phase HPLC. Crude cyclic peptide (1.0 g) was dissolved in 0.25 M triethylammonium phosphate (50 mL) buffer, pH 2.25 (TEAP 2.25), containing acetonitrile and purified according to published procedures.[13] Peptide was loaded onto a preparative reversed-phase HPLC cartridge (5 × 30 cm) packed with Vydac C_{18} silica (15–20-μm particle size) (The Separations Group, Hesperia, CA). The peptide was eluted under gradient conditions (50–70% B in 60 min), with solvent A being TEAP 2.25 and solvent B being 60% acetonitrile and 40% A, at a flow rate of 100 mL/min. Analytical control of individual fractions was carried out using reversed-phase analytical HPLC (Vydac C_{18}) under isocratic conditions (62% B, retention time 3.8 min). The selected fractions were diluted (1:1) with water and further purified preparatively using different solvents, A (0.1% TFA) and B (60% acetonitrile/40% A), under gradient conditions (30–70% B in 40 min). Selected fractions were lyophilized to yield 230 mg of cyclic peptide of high purity. The observed mass spectral value of 1415.8 for the monoisotopic protonated molecular ion was in agreement with the calculated value of 1415.7. $[\alpha]_D$ is −76° (c = 1 in AcOH).

Nuclear Magnetic Resonance. Most NMR studies were performed on a 5.4 mM solution of the Asp4-Dpr10 analogue in $CDCl_3$/DMSO-d_6 (5:1 (v/v)) (0.7-mL total volume). The ^{13}C longitudinal relaxation time measurement was carried out in the same solvent system with a 10 mM sample of the peptide. Some spectra were run on a 5 mM solution of the Asp4–Dpr10 analogue in DMSO-d_6. Deuterated solvents were "100 atom % D", from Sigma Chemical Co. The dimethyl sulfoxide resonance was used as an internal reference (2.49 ppm), and chemical shifts are given relative to this signal.

The NMR spectra were recorded on a Varian VXR 500 spectrometer operating at a 500-MHz proton frequency. Sequential resonance assignments were obtained by using two-dimensional total correlation spectroscopy (TOCSY),[14] two-dimensional correlated spectroscopy (COSY),[15] and two-dimensional nuclear Overhauser spectroscopy (NOESY).[16] Coupling constants were measured on resolution-enhanced one-dimensional spectra recorded at 25, 33, and 41 °C, and on a two-dimensional J-resolved spectrum[17] obtained at 25 °C.

The COSY spectrum was recorded at 25 °C in the absolute value mode, with 6000-Hz spectral width in both dimensions and 1024 complex points for each t_1 value. There were 256 t_1 measurements of 32 transients each, with a 1-s relaxation delay. The data were processed using the Varian VNMR software. An unshifted sine bell function was used in both dimensions, and a data matrix of 1024 × 1024 points was obtained by zero filling.

The NOESY and TOCSY NMR spectra were recorded in the phase-sensitive mode.[18] For all of them, 2 × 256 free induction decays were obtained containing 1024 complex points each. The sweep width was 7500 Hz in both dimensions, and the residual water peak was suppressed by very low power gated irradiation at its observed resonance frequency. NOESY spectra for qualitative purposes were recorded at 0, 25, and 50 °C, with a 0.3-s mixing time and 1-s relaxation delay. NOESY spectra for interproton distance measurements were obtained at 25 °C, with 0.1-, 0.125-, 0.2-, 0.3-, and 0.4-s mixing times, a 2-s relaxation delay, and 64–96 transients per t_1 value. Several TOCSY spectra were collected at temperatures ranging from 9 to 41 °C; a 5-kHz spin-lock field, a mixing time of 75 ms, and a trim pulse of 1 ms were used in all cases, with a 1-s relaxation delay and 16 or 32 transients per t_1 value. The phase-sensitive data were processed on a SUN 4/260 computer, using the FTNMR program developed by Dennis Hare (Hare Research Inc.). In general, Gaussian or sine bell apodization functions were used in both dimensions, and a matrix of 1024 × 1024 real points was formed by zero filling. First point multiplication of the FIDS in the t_1 dimension by 0.5 was performed before the Fourier transform along this dimension.[19] Some two-dimensional data sets were symmetrized about the diagonal, although unsymmetrized data were carefully examined to verify that no artifacts were introduced by symmetrization. A 90°-shifted sine bell was used to process the quantitative NOESY spectra. Polynomial baseline correction of different orders produced small oscillations of the baseline (probably due to the particular characteristics of the spectra) which were inadmissible to integrate the cross-peak volumes in the shorter mixing time data. For these spectra, multiplication of the first point of the FIDs by an experimentally determined factor, prior to the Fourier transformation in both dimensions,[19] was used to align the baseline with the zero intensity level. This method clearly improved the reliability of the volume integrals and the agreement between volumes of symmetric cross-peaks. The factors used were around 1.2–1.3 and 0.6–0.7 in the t_2 and t_1 dimensions, respectively. Volumes were integrated at both sides of the diagonal of the nonsymmetrized spectra using the FTNMR program routines.

Results and Discussion

Assignment of Proton Resonances. The 500-MHz ^{1}H NMR spectrum of the Asp4–Dpr10 analogue in $CDCl_3$/DMSO-d_6 (5:1 (v/v)) is shown in Figure 2. Severe overlapping is observed in the low-field region of the spectrum due to the presence of four different aromatic residues. The resonances that can be initially assigned in the spectrum are the Ac0 methyl, the D-Trp3 NHε, the Leu7 δ-methyls, and the Δ^3-Pro1 α,β,γ-spin system. The small signals near these resonances indicate the presence of two other slowly interconverting conformers accompanying the major form of this molecule (most likely due to cis/trans isomerization about the Xxx-Pro peptide bonds, as explained below).

All the proton resonances of the Asp4–Dpr10 analogue were assigned through the combined use of the 500-MHz TOCSY,

(13) Rivier, J. E.; McClintock, R.; Galyean, B.; Anderson, H. *J. Chromatogr.* **1984**, *288*, 303–328.
(14) Davis, D. G.; Bax, A. *J. Am. Chem. Soc.* **1985**, *107*, 2821–2823.
(15) (a) Aue, W. P.; Bartholdi, E.; Ernst, R. R. *J. Chem. Phys.* **1976**, *64*, 2229–2246. (b) Nagayama, K.; Kumar, A.; Wüthrich, K.; & Ernst, R. R. *J. Magn. Reson.* **1980**, *40*, 321–334. (c) Bax, A. *Two-Dimensional Nuclear Magnetic Resonance in Liquids*; Reidel: Boston, 1982.
(16) (a) Jeener, J.; Meier, B. H.; Bachmann, P.; Ernst, R. R. *J. Chem. Phys.* **1979**, *71*, 4546–4553. (b) Kumar, A.; Wagner, G.; Ernst, R. R.; Wüthrich, K. *J. Am. Chem. Soc.* **1981**, *103*, 3654–3658. (c) Macura, S.; Huang, Y.; Suter, D.; Ernst, R. R. *J. Magn. Reson.* **1981**, *43*, 259–281.
(17) Nagayama, K.; Wüthrich, K.; Bachmann, P.; Ernst, R. R. *Biochem. Biophys. Res. Commun.* **1977**, *78*, 99–105.
(18) States, D. J.; Haberkorn, R. A.; Ruben, D. J. *J. Magn. Reson.* **1982**, *48*, 286–292.
(19) Otting, G.; Widmer, H.; Wagner, G.; Wüthrich, K. *J. Magn. Reson.* **1986**, *66*, 187–193.

Table I. ^{1}H Chemical Shifts for the Asp4–Dpr10 Analogue in $CDCl_3$/DMSO-d_6 (5:1 (v/v))[a]

residue	NH	Hα	Hβ1	Hβ2	others
AcO					CH_3 1.96
Δ^3-Pro1		4.97	5.36		Hγ 5.81, Hδ1 4.27, Hδ2 4.13
D-*p*FPhe2	8.47	4.30	2.98[b]	2.69[c]	$H\delta_2$ 6.99, $H\epsilon_2$ 6.75
D-Trp3	7.84	4.51	3.23[b]	3.13[c]	Hδ1 7.05, Hε3 7.49, Hζ2 7.29, Hζ3 6.91, Hη2 7.01, NHε1 10.17
Asp4	7.61	4.62	2.64[b]	2.30[c]	
Tyr5	7.68	4.24	2.86	2.78	$H\delta_2$ 6.84, $H\epsilon_2$ 6.62, OHη 7.05
D-2Na16	8.03	4.50	3.06[d]		Hδ1 7.56, Hδ2 7.25, Hε2 7.64, Hζ1/Hη2 7.67, Hη1/Hθ 7.33
Leu7	8.08	4.07	1.47	1.38	Hγ 0.86, $H\delta1_3$ 0.50, $H\delta2_3$ 0.48
Arg8	7.56	4.50	1.82	1.60	$H\gamma_2$ 1.51, $H\delta_2$ 3.03, NHε 7.38, $NH\eta1_2$ 7.04, $NH\eta2_2$ 6.79
Pro9		4.34	2.04	1.81	Hγ1 1.94, Hγ2 1.81, Hδ1 3.79, Hδ2 3.50
Dpr10	8.04	4.53	3.73[b]	3.24[c]	NHγ 7.43
NH_2					NH_2^2 7.32, NH_2^1 6.47

[a] Chemical shifts relative to the DMSO resonance (2.49 ppm); temperature 25 °C; uncertainty ±0.02 ppm. [b] Pro-*R*. [c] Pro-*S*. [d] Hβ protons magnetically equivalent.

Table II. Accessibility of the Amide Protons of the Asp4–Dpr10 Analogue

amide proton	$\Delta\delta/\Delta T$[a]	$\Delta\delta/\Delta$solv[b]
D-*p*FPhe2 NH	7.1	−0.13
D-Trp3 NH	4.1	0.20
D-Trp3 NHε	4.4	0.63
Asp4 NH	1.2	0.43
Tyr5 NH	2.2	0.08
D-2Na16 NH	3.9	0.69
Leu7 NH	3.8	0.26
Arg8 NH	0.7	0.09
Arg8 NHε	0.4	0.13
Dpr10 NH	3.9	−0.14
Dpr10 NHγ	2.9	0.15
NH_2^1	5.4	*c*
NH_2^2	4.7	*c*

[a] $\Delta\delta/\Delta T$ in $CDCl_3$/DMSO-d_6 (5:1 (v/v)) (ppb/K). [b] δ[$CDCl_3$/DMSO-d_6 (5:1 (v/v))] − δ[DMSO-d_6] (ppm). [c] Not determined.

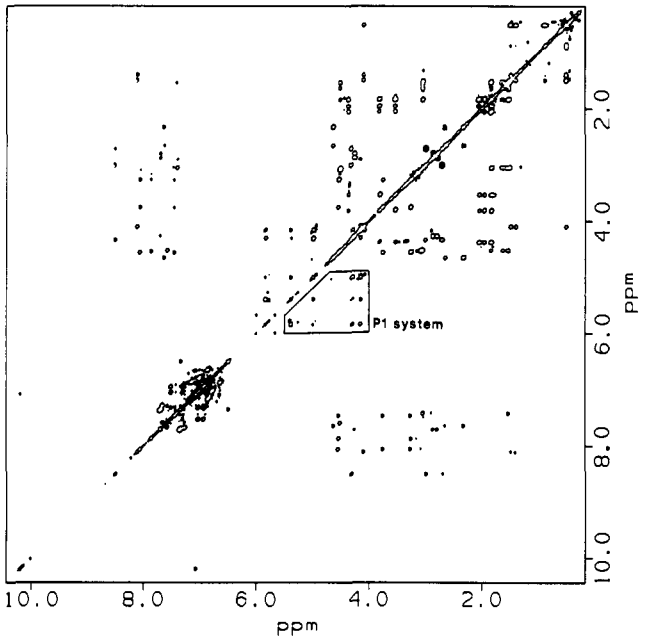

Figure 3. Contour map of a 500-MHz ^{1}H phase-sensitive TOCSY spectrum of the Asp4–Dpr10 GnRH analogue in $CDCl_3$/DMSO-d_6 (5:1 (v/v)) at 25 °C. The correlation peaks corresponding to the Δ^3-Pro1 spin system are indicated.

COSY, and NOESY spectra (Table I). The correlations corresponding to Δ^3-Pro1, whose whole spin system is readily identified in the TOCSY spectrum (Figure 3), can be used as a starting point for the sequential assignment process.[20] In Figure 4 is shown

(20) Wüthrich, K. *NMR of Proteins and Nucleic Acids*; John Wiley and Sons: New York, 1986.

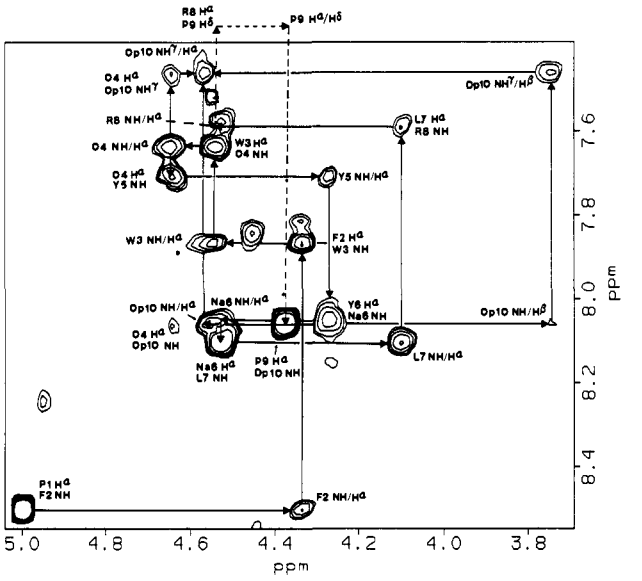

Figure 4. Contour map of the region connecting amide and Hα protons in a 500-MHz ^{1}H phase-sensitive NOESY spectrum of the Asp4–Dpr10 GnRH analogue. Cross-peaks within a residue are also observed in the TOCSY spectrum. The pathway followed to assign sequentially all the backbone protons of the molecule is illustrated. The pathway is bifurcated in the Asp4 NH/H$^\alpha$ cross-peak, in accordance with the branching of the peptidic backbone, and closed following either of two directions due to the cyclic nature of the molecule.

Table III. Coupling Constants for the Asp4–Dpr10 Analogue in $CDCl_3$/DMSO-d_6 (5:1 (v/v))[a]

	D-*p*FPhe2	D-Trp3	Asp4	Tyr5	Leu7	Dpr10
$^3J_{HN\alpha}$	7.5	6.9			8.2	8.0
$^3J_{\alpha\beta1}$	4.7	5.5	4.2[b]	6.4		
$^3J_{\alpha\beta2}$	10.0	9.1	8.4[b]	7.8		

[a] Several couplings could not be measured because of broad lines and/or overlapping; uncertainty ±0.3 Hz. [b] Determined at 41 °C, where lines were sufficiently sharp.

the assignment pathway, which is bifurcated in the Asp4 NH/Hα cross-peak, in accordance with the branching of the peptidic backbone, and is closed following either of both directions due to the cyclic structure of the molecule. All the amide and aliphatic resonances were identified in this process. The cross-peak patterns in the aromatic region of the TOCSY and NOESY spectra, and the NOESY correlations with the corresponding Hα and Hβ protons, allowed the assignment of all the aromatic signals. The Dpr10 $CONH_2$ protons were identified through the strong cross-peak between them and correlations with other protons in this residue that appear in the NOESY spectrum. Finally, tentative assignments for the labile protons Tyr5 OH and Arg8 guanidino were confirmed through their respective correlations with Tyr5 Hε and Arg8 side chain protons in a NOESY spectrum run at 0 °C.

Table IV. Interproton Distances Measured by NMR for the Asp4–Dpr10 Analogue in $CDCl_3$/DMSO-d_6 (5:1 (v/v))[a]

interproton distance	measured value	limits	interproton distance	measured value	limits
		Fixed Distances			
F2 Hβ1/Hβ2[b]	1.81	1.75	W3 Hε3/Hζ3	2.46	2.49
D4 Hβ1/Hβ2[b]	1.76	1.75	W3 NHε1/Hδ1	2.57	2.64
P9 Hδ1/Hδ2[b]	1.71	1.79	W3 NHε1/Hζ2	2.96	2.83
Dp10 Hβ1/Hβ2[b]	1.76	1.75	Na6 Hδ2/Hε2	2.55	2.43
P1 Hβ/Hγ	2.60	2.58			
		Distances Involving Backbone and Hβ Protons			
P1 Hα/F2 NH	2.3	2.1–2.5*	Y5 Hα/Hβ1	2.5	2.2–2.8
F2 NH/Hα	2.9	2.6–3.1*	Y5 Hα/Hβ2	2.5	2.2–2.8
F2 NH/Hβ1	3.0	2.7–3.4	Y5 Hα/Na6 NH	2.5	2.3–2.7*
F2 NH/Hβ2	2.8	2.5–3.2	Na6 NH/Hα	2.5[c]	
F2 Hα/Hβ1	2.4	2.2–2.7	Na6 NH/Hβ	2.9[d]	
F2 Hα/Hβ2	2.6	2.3–2.9	Na6 Hα/Hβ	2.6[d]	
F2 Hα/W3 NH	2.6	2.4–2.9*	Na6 Hα/L7 NH	2.2	2.0–2.4*
F2 NH/W3 NH	2.8	2.5–3.1*	Na6 Hβ/L7 NH	3.0[d]	
W3 NH/Hα	2.6	2.4–2.9*	L7 NH/Hα	2.6	2.4–2.9*
W3 NH/Hβ1	2.9	2.6–3.2	L7 NH/R8 NH	2.5	2.3–2.8*
W3 NH/Hβ2	2.6	2.3–2.9	L7 Hα/R8 NH	3.1	2.8–3.4*
W3 Hα/Hβ1	2.4	2.2–2.7	R8 NH/Hα	3.0[c]	
W3 Hα/Hβ2	2.6[c]		R8 Hα/P9 Hδ1	2.2	2.0–2.5*
W3 Hα/D4 NH	2.4	2.2–2.6*	R8 Hα/P9 Hδ2	2.3	2.0–2.5*
D4 NH/Hα	2.7	2.5–3.0*	P9 Hα/Dp10 NH	2.2	2.0–2.4*
D4 NH/Hβ1	3.0	2.6–3.4	P9 Hβ2/Dp10 NH	2.9	2.6–3.2
D4 NH/Hβ2	2.6	2.3–3.0	Dp10 NH/Hα	2.8[c]	
D4 Hα/Hβ1	2.6	2.3–2.9	Dp10 NH/Hβ1	3.1	2.8–3.4
D4 Hα/Hβ2	2.6	2.3–2.9	Dp10 NH/Hβ2	2.9	2.6–3.2
D4 Hα/Y5 NH	2.5	2.3–2.7*	Dp10 NH/NHγ	2.9	2.6–3.2*
D4 Hα/Dp10 NH	3.4	3.0–3.9	Dp10 Hα/Hβ1	2.3	2.1–2.6
D4 Hα/Dp10 NHγ	3.0	2.7–3.4	Dp10 Hα/Hβ2	2.9[c]	
D4 Hβ1/Dp10 NHγ	2.7	2.5–3.0	Dp10 Hα/NHγ	2.8	2.5–3.1*
D4 Hβ2/Dp10 NHγ	2.7	2.5–3.0	Dp10 Hα/NH_2[2]	2.9	2.6–3.2
Y5 NH/Hα	2.7	2.4–3.0*	Dp10 Hβ1/NHγ	2.9	2.6–3.2
Y5 NH/Hβ1	2.9	2.6–3.2	Dp10 Hβ2/NHγ	2.7	2.4–3.0
Y5 NH/Hβ2	2.8	2.5–3.1			
		Distances between Aliphatic and Aromatic Protons			
W3 Hα/Hδ1	3.5	3.0–4.0	Y5 Hβ1/Hδ	2.8	2.4–3.2
W3 Hα/Hε3	2.8	2.4–3.2	Y5 Hβ2/Hδ	2.8	2.4–3.2
W3 Hβ1/Hδ1	3.3	2.9–3.7	Na6 Hα/Hδ1	2.6	2.3–3.0
W3 Hβ2/Hδ1	3.2	2.6–3.6	Na6 Hα/Hδ2	2.8	2.4–3.2
W3 Hβ1/Hε3	2.8	2.4–3.2	Na6 Hβ/Hδ1	3.0[d]	
W3 Hβ2/Hε3	2.9	2.5–3.3	Na6 Hβ/Hδ2	2.9[d]	
Y5 Hα/Hδ	2.8	2.4–3.2			

[a] All distance values in angstroms. The theoretical values are given for the fixed distances, instead of distance ranges estimated from the data. The methodology used to obtain the distances and their limits is explained in the text. An asterisk after the limits indicates those that could be used as restraints, in a first approach, in restrained molecular dynamics calculations (see following paper in this issue). Abbreviations are as indicated in the legend of Figure 1. [b] Interactions used to obtain reference volumes. [c] Overlapping only allows a rough estimate. [d] Average value calculated assuming that the distance to both Na6 Hβ protons is the same.

Conformationally Relevant NMR Parameters. The sensitivity of the amide proton chemical shifts to the temperature and the coupling constants measured for the Asp4–Dpr10 analogue are summarized in Tables II and III, respectively. A series of five TOCSY spectra between 9 and 41 °C were recorded to obtain the temperature coefficients of the NH resonances in $CDCl_3$/DMSO-d_6 (5:1 (v/v)). The changes of the chemical shifts with temperature are linear, suggesting that no major conformational rearrangements occur in the temperature range studied. The resonances that show smallest variation with temperature are the ones corresponding to the Asp4, Tyr5, and Arg8 NH's. All of these protons show relatively low field chemical shift (7.56–7.68 ppm) and can be proposed to be involved in intramolecular hydrogen bonds. The Dpr10 NHγ seems also somewhat sequestered from the solvent. The fact that all the other, more exposed, NH's show even lower field chemical shifts (7.84–8.47 ppm) is explained by their exposure to the strong hydrogen bond acceptor DMSO-d_6 present in the solvent mixture.

Coupling constants between vicinal protons were obtained from a J-resolved spectrum and from resolution-enhanced one-dimensional spectra at 25–41 °C (Table III). The line width of some amide resonances and/or their overlapping with the aromatic signals prevented the measurement of several $^3J_{HN\alpha}$ coupling constants and couplings involving Dpr10 Hβ protons. Limited information was thus obtained from these data. Coupling constants between Hα and Hβ protons for some residues were used, together with NOE data, to obtain stereospecific assignments of Hβ protons in these residues, and to determine the preferred rotamers in some of their side chains (see below).

NOE Data. Measurement of Interproton Distances. Nuclear Overhauser effects (NOEs) are the most informative NMR parameters to deduce the three-dimensional structure of peptides, as they can be related, with certain assumptions, to the distance between the interacting nuclei. To obtain interproton distances for the Asp4–Dpr10 analogue (Table IV), we recorded a series of NOESY spectra with 0.1-, 0.125-, 0.2-, 0.3-, and 0.4-s mixing times. The interproton distances were calculated primarily from the data obtained with the first two mixing times, assuming the two-spin approximation in its linear extrapolation (r^{-6} proportional to the volume integral of the cross-peaks). The linear approximation was clearly not valid in the 0.2- and 0.3-s mixing time data for the strongest interactions, but it held for the longer distances; these data, where the volume integrals are larger and more accurate, were also used to quantitate the weaker interactions. The data at 0.4-s mixing time were not used in the interproton distance measurements, as a general decrease in the intensities of the NOEs, with respect to the 0.3-s mixing time data, was observed. A weighted average of the volume integrals corresponding to the

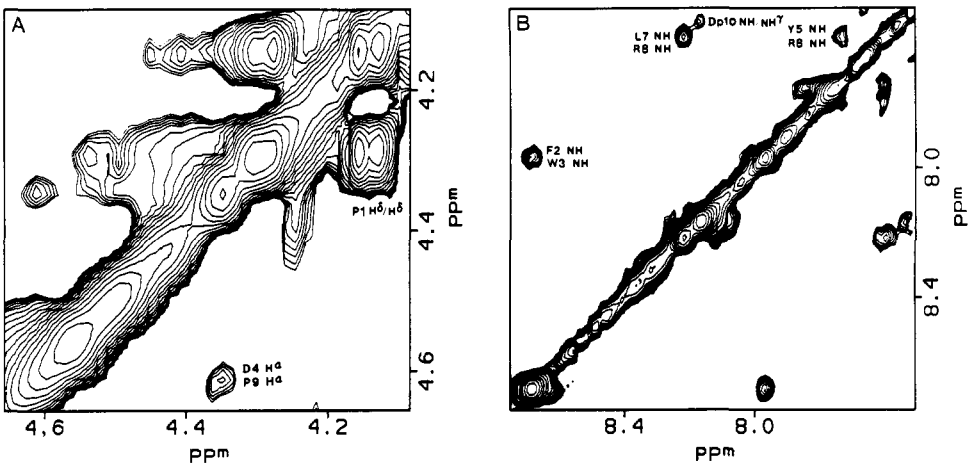

Figure 5. Contour maps corresponding to different regions of an unsymmetrized NOESY spectrum of the Asp4–Dpr10 analogue (0 °C, 300-ms mixing time): (A) part of the aliphatic/aliphatic region where an Asp4 Hα/Pro9 Hα NOE can be observed, (B) part of the amide/amide region where four NH/NH interactions can be observed.

geminal interactions between D-*p*FPhe2, Asp4, and Dpr10 Hβ and Pro9 Hδ protons was used as a reference, assuming interproton Hβ/Hβ and Hδ/Hδ distances of 1.75 and 1.79 Å, respectively. Interproton distances were calculated independently on each side of the diagonal of the relevant NOESY spectra, using the corresponding reference volume; for the 0.2- and 0.3-s mixing time NOESYs, the reference volumes of the 0.1-s mixing time NOESY (run back to back with them) were used, dividing all volumes by the corresponding mixing time.

The interproton distances shown in Table IV correspond to averages of the different values calculated for each interaction. The values obtained for protons whose interproton distance is fixed (aromatics and Δ^3-Pro1 Hβ/Hγ) give an idea of the quality of the data. The distance limits indicated are error estimates based on the intrinsic error associated with the methodology[21] and the dispersion in the different values obtained for each distance. The errors for some distances are very likely smaller than the indicated ranges, but it was considered appropriate to keep the bounds at about ±10% of the measured distances, to apply them as restraints in molecular dynamics calculations (see following paper in this issue). We adopted this criterion considering that even if the distances correspond to a single major conformation of the peptide, a margin has to be left for the natural molecular motions and for small structural rearrangements. Many of the distances measured probably correspond to averaged local conformations, especially those involving side chain protons, but they were quantitated to help in the stereospecific assignment of Hβ protons, determination of preferred rotamers, or assessment of free rotation of aromatic rings. We consider that only the 19 interproton distances indicated with an asterisk in Table IV should be used, at least in a first approach, as restraints for molecular dynamics simulations. NOEs within the side chains with the most complicated spin systems (Leu7, Arg8, and Pro9) were not quantitated. A final point to note is that the interproton distances have been calculated assuming a single motional correlation time for all the protons of the peptide. This could be, a priori, in contradiction with the existence of different mobilities in distinct parts of the molecule, which is proposed later. To address this issue, we measured ^{13}C longitudinal relaxation times for the Asp4–Dpr10 analogue in $CDCl_3$/DMSO-d_6 (5:1 (v/v)) (data not shown). Although there is some variability in the NT_1 values measured, the error introduced in the interproton distances by differences in mobility should be within the limits indicated in Table IV.

As can be observed in Table IV, all the interproton distances measured correspond to correlations within a residue or between neighboring residues. Longer range interactions are much more informative, in general, to define the overall folding of a polypeptide chain. Unfortunately, only two such interactions could be observed, one between the Asp4 Hα and Pro9 Hα protons (Figure 5a), and another between Tyr5 NH and Arg8 NH (Figure 5b, where also the existing NH_i/NH_{i+1} correlations can be observed). Both interactions were observed at room temperature, but were better assessed at 0 °C. It will be seen that although these two interactions could not be quantitated due to their proximity to the diagonal, they were very helpful to define the conformation of the ring portion of the molecule (residues 4–10) and the orientation of the tail (formed by residues 1–3) with respect to the ring.

Conformational Analysis. The major form of the Asp4–Dpr10 analogue in $CDCl_3$/DMSO-d_6 (5:1 (v/v)) is the all-trans conformer, as is demonstrated by the observation of NOE interactions between the Ac0 CH_3 and Δ^3-Pro1 Hδ protons, and between the Arg8 Hα and Pro9 Hδ protons, and by all the sequential $H\alpha_i/NH_{i+1}$ connectivities. A NOESY spectrum recorded at 50 °C shows exchange cross-peaks between the major form of the peptide and the minor components, which demonstrates that they correspond to other conformers of the Asp4–Dpr10 analogue. Although assignments could not be obtained for the second conformer, an Ac0/Δ^3-Pro1 Hα NOE interaction could be assessed at 0 °C showing that this conformer contains a cis Ac0/Δ^3-Pro1 amide bond. Whether the least abundant species contains a cis Arg8/Pro9 peptide bond could not be assessed.

The parameters described in the last two sections, together with model building and standard structural considerations,[20] allow the development of a model for the conformation of the all-trans form of the peptide (Figure 6). A type II′ β turn with D-2Nal6 and Leu7 in the corner positions, closed by a hydrogen bond between Arg8 NH and Tyr5 CO, and favored by the heterochiral DL sequence, is a well-defined feature of the model. The proposal of this turn is supported by the low-temperature dependence of the Arg8 NH chemical shift, by the short Leu7 NH/Arg8 NH and 2Nal6 Hα/Leu7 NH distances, and by the long Leu 7 Hα/Arg8 NH distance. The large value of the Leu7 $^3J_{HN\alpha}$ (8.2 Hz) is also in agreement with the existence of this type II′ β turn.[22] Model building illustrates how a transannular hydrogen bond between Tyr5 NH and Arg8 CO can easily be formed, leading to a structure similar to a β-hairpin, with Tyr5 and Arg8 in an extended conformation (Figure 6). The low-temperature coefficient of the Tyr5 NH and the NOESY pattern in the region agrees with this conformational feature, which is strongly supported by the transannular Tyr5 NH/Arg8 NH and Asp4 Hα/Pro9 Hα NOEs.

The most challenging part of the conformational analysis of the Asp4–Dpr10 analogue is to determine if the linear part of the peptide, the tail formed by residues 1–3, exists in a major structural

(21) Clore, G. M.; Gronenborn, A. M. *J. Magn. Reson.* **1985**, *61*, 158–164.

(22) Aubry, A.; Chung, M. T.; Marraud, M. *J. Am. Chem. Soc.* **1985**, *107*, 7640–7647.

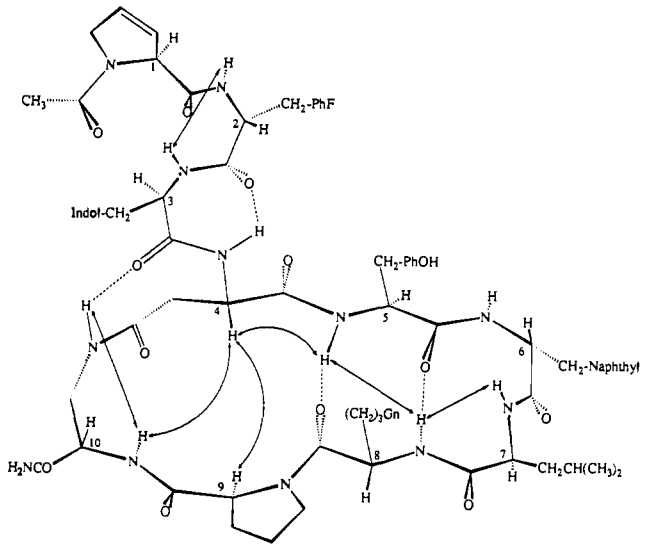

Figure 6. Perspective drawing of the conformational model proposed for the Asp4–Dpr10 GnRH analogue (Gn indicates the guanidino group of the Arg8 side chain). The model is supported by the NMR data presented here and the molecular dynamics simulations described in the following paper in this issue. The positions of the Cα carbons have been labeled with the corresponding residue number. Dashed lines indicate hydrogen bonds, straight arrows indicate NH/NH NOE interactions, and curved arrows indicate three critical NOEs involving Asp4 Hα that define the orientation of the tail with respect to the ring. A β-hairpin structure in residues 5–8, including two transannular hydrogen bonds (Tyr5 NH/Arg8 CO and Arg8 NH/Tyr5 CO) and a type II′ β turn around D-2Nal6-Leu7, is a well-defined feature of the molecule. The tail formed by residues 1–3 is oriented above the ring. A γ turn around D-Trp3, with a hydrogen bond between Asp4 NH and D-*p*FPhe2 CO, is likely to exist. Residues 1 and 2 appear to be visiting several conformations; a type II β turn around these residues could be formed frequently. The Asp4–Dpr10 bridge also presents conformational averaging; a Dpr10 NHγ/D-Trp3 CO hydrogen bond is proposed for some of the preferred conformations of the bridge. Note the location of the Tyr5 and Arg8 side chains above the ring, which suggests the likelihood of interactions between these side chains, and between them and the tail.

family, and with a definite orientation with respect to the ring, or interconverts among several conformations. The lack of NOE interactions between the tail and the ring makes it difficult to define the tail orientation, but the NOE interactions of Asp4 Hα with Tyr5 NH, Pro9 Hα, and Dpr10 NH, together with the β-hairpin structure, strongly indicate that the Asp4 N–Cα bond is pointing above the ring (Figure 6). The intermediate values of the backbone interproton distances and the $^3J_{HN\alpha}$ coupling constants in the tail are suggestive of significant conformational averaging, but it also seems possible to fit them into a single reasonable structure. The D-*p*FPhe2 NH/D-Trp3 NH NOE and the low-temperature dependence of the Asp4 NH indicate, on the other hand, the presence of structure in the tail. The NH/NH NOE could imply the presence of a type II β-turn conformation around Δ^3-Pro1 and D-*p*FPhe2 (Figure 6), favored by the heterochiral LD sequence. However, this is not reflected in a low-temperature coefficient for D-Trp3 NH. Furthermore, the interproton distances involved in this region do not fit with the ones expected for a type II β turn, but agree with the possibility of a significant population of turn structures in the conformational space visited by residues 1 and 2. With regard to the low-temperature dependence of Asp4 NH, a γ-turn conformation around D-Trp3, closed by an Asp4 NH/D-*p*FPhe2 CO hydrogen bond (Figure 6), is compatible with the interproton distances measured, and with the $^3J_{HN\alpha}$ of D-Trp3. The D-Trp3 Cβ resonance can be assigned in the ^{13}C spectrum at 26.2 ppm; the 1.7 ppm upfield shift with respect to literature values for reference peptides[23] is consistent with the D-Trp3 Cβ and CO being eclipsed, which is characteristic of γ turns.[24]

The β-hairpin structure around residues 5–8 and the orientation of the tail above the ring bring an overall fold for the Asp4–Dpr10 analogue that has clear similarities with the structure determined for the parent cyclo(1–10) decapeptide GnRH antagonist.[10] This point is better illustrated in the following paper in this issue, but it is clear from model building that the Tyr5 and Arg8 side chains can be easily oriented above the ring as a consequence of the β-hairpin structure (Figure 6). Hence, interactions between these side chains are likely to exist, and also between them and the tail formed by residues 1–3. The possibility of these interactions suggests additional bridges that could be introduced in the molecule to obtain more constrained GnRH antagonists.

Side Chain Conformations. It is generally reasonable to assume that the side chains of small peptides have high mobility, but they are mainly populating the staggered rotamers. When $^3J_{\alpha\beta}$ coupling constants are available, they can be combined with NOE data (NH/Hβ and Hα/Hβ interactions) to obtain stereospecific assignments for the Hβ protons,[25] and then used to calculate populations of rotamers, with the χ_1 torsion angle taking the values −60°, 180°, and 60°.[26] Adapting the referenced schemes to treat D-amino acids, we obtained stereospecific assignments for the D-*p*FPhe2 and D-Trp3 Hβ protons (Table I) and determined that the preferred rotamer for the side chains of both residues is the one with χ_1 = 60, with calculated populations of about 70% and 60%, respectively. The corresponding interproton distances and $^3J_{\alpha\beta}$ coupling constants for Tyr5 present averaged values, which indicates that the three rotamers have similar populations in this case. The assessment of the rotameric populations in D-2Nal6 is hindered by the magnetic equivalence of the Hβ protons in this residue, but the NOE data suggest that if there is any preferred rotamer, this should be the one with χ_1 = 60°. This is concluded from the Hα/Ar distances and the averaged distance between the Hβ protons and Leu7 NH (Table IV). The bounds for the possible distances between Hα and Hδ1 or Hδ2 are 2.0–4.7 Å for χ_1 = 60° and 180°, while they are 3.5–4.9 Å for χ_1 = −60°, which excludes this last value of χ_1 for a preferred conformer. The presence of an NOE between the Hβ and Leu7 NH is incompatible, on the other hand, with a preference for the rotamer with χ_1 = 180°, as the minimum D-2Nal6 Hβ/Leu7 NH distance would be around 4.2 Å. The preference of the D-residues for the χ_1 = 60° rotamer is consistent with the higher propensity to populate the χ_1 = −60° rotamer observed for L-residues in proteins.[27] On the other hand, the coexistence of similar populations of the three rotamers in Tyr5 is somewhat uncommon. The χ_1 = 60° rotameric state is usually the least populated, due to steric reasons, but is the rotamer that better orients the Tyr5 side chain above the ring and could be stabilized by electrostatic interactions with the Arg8 side chain and/or the amide groups of the tail, which were mentioned earlier (see also following paper in this issue). The likelihood of these interactions is also supported by the observation of a weak Arg8 Hγ/Pro9 Hδ2 NOE (not shown). Model building and analysis of the corresponding interproton distances in the molecular dynamics structures of the Asp4–Dpr10 analogue described in the following paper indicates that this NOE should be originated when the Arg8 side chain is oriented toward the tail and the Tyr5 side chain.

The Asp4 and Dpr10 side chains are linked to bring about the cyclic structure of the Asp4–Dpr10 analogue, and hence, it is more likely that they present well-defined conformations, dictated by the structure of the remaining residues in the ring, and perhaps with higher deviations from the staggered rotamers. However, some flexibility can be expected around the Asp4–Dpr10 bridge

(23) Wüthrich, K. *NMR in Biological Research: Peptides and Proteins*; North-Holland: Amsterdam, The Netherlands; American Elsevier: New York, 1976.

(24) Siemion, I. Z.; Wieland, T.; Pook, K. H. *Angew. Chem.* **1975**, *87*, 712–714.

(25) (a) Wagner, G.; Braun, W.; Havel, T. F.; Schaumann, T.; Go, N.; Wüthrich, K. *J. Mol. Biol.* **1987**, *196*, 611–639. (b) Hyberts, G.; Marki, W.; Wagner, G. *Eur. J. Biochem.* **1987**, *164*, 625–635.

(26) (a) Demarco, A.; Llinas, M.; Wüthrich, K. *Biopolymers* **1978**, *17*, 617–636. (b) Cung, M. T.; Marraud, M. *Biopolymers* **1982**, *21*, 953–967.

(27) Ponder, J. W.; Richards, F. M. *J. Mol. Biol.* **1987**, *193*, 775–791.

due to the presence of a methylene group on each side of the amide linkage. Indeed, computer graphics shows very clearly that the interproton distances in this region of the molecule cannot be fit by a single conformation. As an example, the distances between Dpr10 NHγ and the two Asp4 Hβ protons can only be equivalent (as observed) when Asp4 χ_2 is near either 0° or 180°; in these cases, values of about 3.3 or 2.2 Å, respectively, are expected for these distances, rather than the measured values (2.7, Table IV). On the other hand, clear broadening of some signals, most of them corresponding to protons close to the Asp4–Dpr10 bridge, is observed in the NMR spectrum. These signals sharpen up very significantly upon increasing the temperature, which suggests the existence of a slow conformational equilibrium in this region of the molecule, with little effect on the conformation of the other side of the ring. Molecular dynamics simulations indicate that, in fact, two different equilibria can be occurring: a fast rotation of the amide bond in the center of the bridge entailing both Asp4 and Dpr10 χ_2 and a slow interconversion between two Asp4 χ_1 rotameric states involving also rearrangements in both χ_2 torsion angles (see following paper in this issue). The best fit to the measured interproton distances and coupling constants implies a predominance of conformations with Asp4 $\chi_1 \approx -80°$, accompanied by a significant population of conformers with Asp4 $\chi_1 \approx -170°$; Dpr10 χ_1 appears to be mostly near −65°. This model yields the stereospecific assignment of the Asp4 and Dpr10 Hβ protons indicated in Table I. Finally, the simulations also indicate that a hydrogen-bonding interaction between Dpr10 NHγ and D-Trp3 CO (Figure 6) is likely to exist for some of the bridge conformations (see following paper), which could explain the relatively low temperature coefficient of this amide proton.

NMR of the Asp4–Dpr10 Analogue in DMSO-d_6. A set of NMR spectra was run on a solution of the Asp4–Dpr10 analogue in DMSO-d_6 to test the sensitivity of its conformation to the environment. Rather than giving a detailed report on these results, we will just summarize the most important observations from these experiments. Two major conformers of the peptide exist in these conditions in a ratio close to 1:1. Most of the resonances in both conformers were assigned, and their identities could be ascertained as the all-trans and one-cis Ac0/Δ^3-Pro1 forms of the peptide. No large differences are observed between the chemical shifts of the aliphatic and aromatic protons of the all-trans conformer in both solvent systems (data not shown). Some differences in the chemical shifts of the amide protons are, on the other hand, worth noting (Table II). The relatively large downfield shift of Asp4 NH (sequestered in $CDCl_3$/DMSO-d_6 (5:1 (v/v)) is somewhat surprising. This observation, together with the small upfield shifts of D-*p*FPhe2 NH and Dpr10 NH in DMSO-d_6, compared to the $CDCl_3$/DMSO-d_6 (5:1 (v/v)) data, suggests a conformational change, as these two protons are not sequestered in the second solvent. A comparison of the amide proton chemical shifts in DMSO-d_6 at 25 and 55 °C gave an idea of their temperature sensitivity in this solvent (data not shown). Both D-*p*FPhe2 NH and Dpr10 NH appear to be somewhat sequestered in DMSO-d_6, and Asp4 NH is exposed, which explains the above observations. The other amide protons which are sequestered in $CDCl_3$/DMSO-d_6 (5:1 (v/v)), Tyr5 NH, Arg8 NH, and Dpr10 NHγ, also seem inaccessible to the solvent in DMSO-d_6, and their chemical shifts show low sensitivity to the change in the solvent (Table II). To these observations we have to add that the NOESY patterns observed in both solvent systems are very similar. It seems most likely, therefore, that the overall structure of the peptide only suffers small rearrangements when the percentage of DMSO-d_6 is raised to 100%; these rearrangements involve mainly hydrogen-bonding interactions, as could be expected when the hydrogen bond donor/acceptor capacity of the solvent is altered.

The structure of the one-cis Ac0/Δ^3-Pro1 form of the Asp4–Dpr10 analogue was not pursued. Nevertheless, it is worth noting that such a "small" change in the molecule produces significant changes in the chemical shifts of many aliphatic protons in the tail and in the Asp4–Dpr10 bridge of the peptide. These changes strongly suggest the presence of structure in the tail, structure that influences the conformation of the bridge. The rearrangement of the tail also seems to affect the Arg8 side chain, whose protons have small, but significant, differences in chemical shifts in the all-trans and the one-cis conformers. This observation suggests that tail/Arg8 side chain interactions are also likely to exist in DMSO-d_6. Overall, the NMR results obtained in DMSO-d_6 support the idea of a quite rigid β-hairpin-like conformation in residues 5–8 of the Asp4–Dpr10 analogue, with a tail oriented above the ring; the tail seems to be sampling some preferred conformations, but is flexible and sensitive to the environment.

Summary

The conformational behavior of a highly potent GnRH antagonist, here referred to as the Asp4–Dpr10 analogue, has been studied by NMR. The existence of regions with different mobility in the molecule makes its conformational analysis difficult, and some of the NMR observations could not have been fully understood without the aid of the molecular dynamics calculations described in the following paper in this issue. Residues 5–8 of the Asp4–Dpr10 analogue adopt a β-hairpin conformation, which includes transannular hydrogen bonds between Tyr5 NH and Arg8 CO and between Arg8 NH and Tyr5 CO. A type II′ β turn around positions 6 and 7 is observed; this turn has been proposed to be essential for biological activity. The measured interproton distances clearly indicated the existence of more than one conformation around the Asp4–Dpr10 bridge. The tail formed by residues 1–3 is oriented above the ring, and its conformation depends on the environment. A γ turn with D-Trp3 in the corner position, closed by a hydrogen bond between Asp4 NH and pFPhe2 CO, seems most likely to exist in $CDCl_3$/DMSO-d_6 (5:1 (v/v)). Residues 1 and 2 could be forming a type II β turn frequently. This conformational model has clear resemblance with the structure found for the parent cyclo(1–10) decapeptide that led to the design of the Asp4–Dpr10 GnRH analogue and suggests new bridging opportunities to create more constrained GnRH analogues.

Acknowledgment. We thank Ron Kaiser, John Porter, Duane Pantoja, and Charleen Miller for technical assistance in the synthesis and characterization of the Asp4–Dpr10 GnRH analogue. J.R. was a fellow from the Ministerio de Educación y Ciencia of Spain. This work was supported by NIH Contract No. NO1-HD-1-3100 and by a grant from the NIH (GM-27616 to L.M.G.). L.M.G. thanks the Robert A. Welch Foundation for continued support.

Registry No. Asp4-Dpr10 analogue, 109001-26-5; linear peptide hydrazide, 139461-69-1.